BioNanoScience (2025) 15:60
https://doi.org/10.1007/s12668-024-01625-4

RESEARCH

Metal and Metal Oxide Nanoparticles: Computational Analysis of Their Interactions and Antibacterial Activities Against *Pseudomonas aeruginosa*

Badr-Edine Sadoq[1] · Somdutt Mujwar[2] · Mohamed Sadoq[3] · Yassir Boulaamane[1] · Mohammed Reda Britel[1] · Adel Bouajaj[1] · Ahmed Touhami[4] · Fakhita Touhami[1] · Amal Maurady[1,5]

Accepted: 7 November 2024

Abstract

The effectiveness of antibiotics against *Pseudomonas aeruginosa* (*P. aeruginosa*) infections is limited by inherent antimicrobial resistance, prompting researchers to seek advanced and cost-effective antibacterial agents. This opportunistic bacterium exhibits drug resistance and regulates its pathogenicity through quorum sensing (QS) mechanisms, suggesting that disrupting these systems could be a promising approach to treating *P. aeruginosa* infections. In this study, we investigated the antibacterial properties of silver nanoparticles (AgNPs), zinc oxide nanoparticles (ZnONPs), and copper oxide nanoparticles (CuONPs) in conjunction with QS systems, focusing on the LasI/R, RhlI/R, and PqsA/PqsR pathways. A computational approach was utilized to examine the interaction patterns between these nanoparticles and QS signaling proteins in *P. aeruginosa* through multiple bioinformatics techniques. The interaction of metals and metal oxides with acyl-homoserine-lactone synthases (LasI, RhlI, PqsA) can impede the binding of precursor molecules, thereby inhibiting the synthesis of functional signaling molecules. Moreover, the binding of nanoparticles to regulatory proteins (LasR, RhlR, PqsR) competes with functional signaling molecules, resulting in a reduced expression of QS-controlled genes. Among the nanoparticles studied, ZnONPs exhibited the highest affinity toward the selected targets. In particular, the PqsA-ZnONPs complex showed stable active binding sites and a high binding affinity (− 3.83 kcal/mol), indicating strong interaction with the active pocket of the pathogen *P. aeruginosa* (PqsA: 5OE3). ZnO nanoparticles demonstrated significant potential as antimicrobial agents against *P. aeruginosa* by disrupting its QS systems. This approach presents a promising direction for developing therapeutic strategies to combat antibiotic-resistant bacteria, including *P. aeruginosa*.

Keywords Antibiotic resistance · Molecular docking · Molecular dynamic simulations · Nanoparticles · *Pseudomonas aeruginosa* · Quorum sensing

1 Introduction

Pseudomonas aeruginosa (*P. aeruginosa*), an opportunistic Gram-negative bacterial pathogen, is responsible for approximately 14% of nosocomial infections in immunocompromised patients [1, 2]. Its persistence, growing antimicrobial resistance, and increased virulence often result in bacteremia, significantly raising the risk of morbidity and mortality in hospitalized individuals [3]. Additionally, the pathogen's inherent ability to form biofilms further exacerbates its antimicrobial resistance [4, 5].

A biofilm constitutes a gathering of microbial cells that forms irreversibly on surfaces, whether biotic or abiotic, enveloped within a self-produced matrix [6]. Incorporating into the extracellular polymeric matrix serves as a survival

✉ Amal Maurady
amaurady@uae.ac.ma

1 Laboratory of Innovative Technologies, National School of Applied Sciences of Tangier, Abdelmalek Essaadi University, Tetouan, Morocco

2 Chitkara College of Pharmacy, Chitkara University, Rajpura 140401, Punjab, India

3 Laboratory of Chemistry and Biology Applied to the Environment, URL-CNRST-N◦13, Faculty of Sciences, Moulay Ismail University, 50050 Meknes, Morocco

4 Department of Physics and Astronomy, University of Texas Rio Grande Valley Edinburg, Brownsville, TX 78520, USA

5 Faculty of Sciences and Techniques of Tangier, Abdelmalek Essaadi University, Tetouan, Morocco

Published online: 05 December 2024

strategy for *P. aeruginosa* amidst environmental fluctuations, aiding in its evasion of host defenses and antimicrobial challenges, thereby heightening the pathogen's virulence [6–8]. Additionally, biofilm formation relies on cell-to-cell communication and signaling that are contingent upon cell density. Quorum sensing (QS) is the most known mechanism for bacterial communication and signaling in which cells produce and react to small chemical signaling molecules called autoinducers [9, 10]. This process enables bacteria to engage in cell-to-cell interactions, facilitating the exchange of information in response to environmental stimuli [11, 12]. As illustrated in Fig. 1, for *P. aeruginosa*, the QS system functions primarily through three distinct pathways: LasI-LasR, RhlI-RhlR, and PqsA-PqsR, all of which are closely interconnected with each other [13, 14]. In reaction to the increase in bacterial cell density, autoinducers N-3-oxododecanoyl-L-homoserine lactone (3O-C12-HSL), N-butanoyl-L-homoserine lactone (C4-HSL), and the Pseudomonas quinolone signal (PQS) are synthesized and bind to their corresponding receptors (LasR, RhlR, and PqsR), thereby orchestrating the transcriptional regulation of target genes [9]. Notably, the synthesis of PQS is regulated by the pqsABCDEH operon, PQS is most abundantly produced during the late stationary phase of growth, acting as a bridge between the Las and Rhl QS systems [15, 16]. The production of extracellular polymeric substances, exotoxin A, lasA protease, lasB elastase, rhamnolipid, lectin, pyocyanin, pyoverdine, and HCN, in *P. aeruginosa* is regulated by QS cascades, which enhance the bacterium's invasiveness [17, 18].

It was reported in previous studies that the malfunction of the QS system reduces the virulence of *P. aeruginosa* and leads to the formation of a vulnerable flat biofilm susceptible to antibiotics [19, 20]. Thus, disrupting the bacterial QS system could be beneficial for treating various diseases, given the pivotal role of QS systems in regulating virulence [21]. Therefore, inhibiting QS is considered a promising strategy to combat *P. aeruginosa* infections [22], as it can effectively prevent biofilm formation, reduce bacterial virulence, and carry a low risk of inducing bacterial resistance. The alarming increase in multidrug-resistance cases highlights the urgent need to explore alternative therapeutic approaches to address biofilm formation and inhibit QS system [10].

The process of QS can be disrupted by targeting different stages of the pathway [23–25]: (i) Inhibiting the biosynthesis of signaling molecules, which are catalyzed by specific enzymes, can block QS by interfering with the activity of these synthetases or the substrates required for signal production. (ii) Degrading signal molecules is another approach that prevents them from reaching the threshold concentration needed to activate QS. (iii) Finally, competitive interference with signal receptors can prevent natural signal molecules from binding, thereby regulating biofilm formation. These mechanisms underscore the importance of QS inhibitors (QSIs) in reducing bacterial virulence and disrupting biofilm formation.

In recent years, many researchers have started using nanotechnology to develop next-generation nano-antimicrobials, including QS nano-inhibitors. For example, metal and metal oxide nanoparticles (NPs) such as silver (AgNPs), zinc oxide (ZnO NPs), and copper oxide (CuO NPs) have been used to combat pathogens [26–29]. These nanoparticles are sometimes combined with traditional antibiotics to increase their effectiveness [30–35]. The antimicrobial properties of nanoparticles can be associated with their ability to degrade signal receptor proteins or inhibit the synthesis of signaling molecules. This leads to a reduction production of virulence factors such as elastase, pyocyanin, and biofilm components in *P. aeruginosa* [36]. These nanoparticles offer numerous advantages, including improved mucus and biofilm penetration, increased solubility, efficient delivery, and sustained activity of QS inhibitors [37].

In the present study, an in-silico analysis was performed to predict the potential binding sites of silver, zinc oxide, and copper oxide nanoparticles on QS-regulated autoinducer

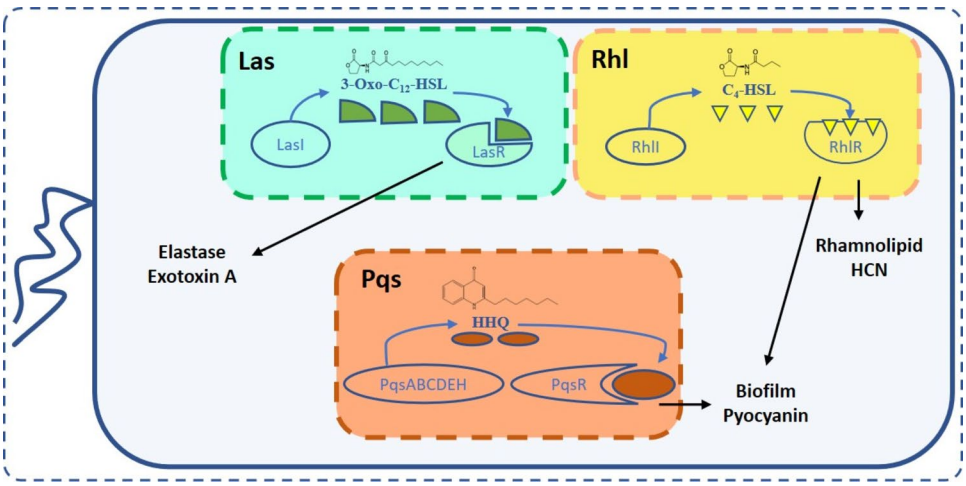

Fig. 1 Schematic diagram of the Las, Rhl, and Pqs QS systems in *P. aeruginosa*. These three major systems use 3-oxo-C12-HSL, C4-HSL, and HHQ/PQS molecules for intercellular communication

synthase proteins (LasI, RhlI, and PqsA) in *P. aeruginosa*. Additionally, the study examined the interactions between these nanoparticles and QS-controlled transcriptional regulatory proteins (LasR, RhlR, and PqsR) to characterize the types of interactions between the nanoparticles and the QS proteins. Finally, molecular dynamics (MD) simulations were conducted to explore the stability of the docked complexes that exhibited the highest affinity throughout the simulation period of 100 ns.

2 Material and Methods

2.1 Selection of Quorum Sensing Proteins in *P. aeruginosa*

The quorum sensing proteins of *P. aeruginosa,* including LasI (acyl-homoserine-lactone synthase), LasR (transcriptional activator protein), PqsA, PqsR (Pseudomonas quinolone signal), RhlI (acyl-homoserine-lactone synthase), and RhlR (transcriptional activator), were selected because of their key roles in QS regulation and the activation of multiple QS pathways, as outlined in the literature [38]. The crystal structures of these proteins were obtained from the Protein Data Bank (LasI, PDB ID 1RO5; LasR, PDB ID 3IX3 chain A; PqsA, PDB ID 5OE3; PqsR, PDB ID 4JVI) and analyzed using AutoDockTools [39]. The LasR protein has two similar chains, A and B, both of which contain co-crystallized ligands.

2.2 Homology Modeling

Homology modeling was used to generate the 3D structures of the RhlI and RhlR proteins. The amino acid sequences of these proteins (UniProtKB IDs P54291 and P54292) were used for structure prediction via Swiss-Model server (http://swissmodel.expasy.org/). Quality assessments were conducted using QMEAN and QMEANDisCo scores [40, 41], and Ramachandran plot assessments were conducted using MolProbity v4.4 [42]. Finally, the overall reliability and additional quality assessment of the protein models were conducted using ERRAT analysis [43].

2.3 Active Site Prediction

The prediction of active site residues within the receptors was conducted using the Prank Web online tool [44] (https://prankweb.cz/). The results were then compared with findings from the literature to confirm accuracy and relevance [45–48].

2.4 PubChem Data for Nanoparticle Structures

The SDF files for silver (PubChem CID: 23,954), zinc oxide (PubChem CID: 14,806), and copper oxide (PubChem CID: 14,829) nanoparticles were obtained from the PubChem database and converted to PDB format using Avogadro [49].

2.5 Molecular Docking Study

The docking was performed using AutoDockTools 1.5.7 software [50]. The dimensions of the GRID box are reported in Table S1, with specific dimensions and centers of each receptor specified in Table S2. A grid spacing of 0.375 Å was set. The ligand–protein interactions were visualized using Discovery Studio Visualizer and PyMOL [51, 52].

2.6 Molecular Dynamic (MD) Simulation

The Desmond program from Schrödinger was utilized to perform 100 ns MD simulations on the quorum-sensing proteins of *P. aeruginosa* with selected nanoparticles that exhibited the highest binding energies. This approach aimed to investigate their binding strengths over time [53, 54]. The TIP3P explicit water model was used to set up an orthorhombic simulation box with a 10 Å distance between the protein-nanoparticle complex and the box walls. Counter ions were added to achieve an isosmotic environment and neutralize charges, maintaining a concentration of 0.15 M NaCl. The system underwent optimization through 2000 iterations with a merging criterion of 1 kcal/mol. Molecular dynamics (MD) simulations were performed on the minimized energy complex system. Temperature and pressure were maintained at 300 K and 1.013 bar, respectively, throughout the simulation. Trajectories were recorded every 9.6 ps, and energy was sampled every 1.2 ps. These trajectories were used to generate simulation diagrams at the end of the simulation.

3 Results and Discussions

3.1 Quality Assessment of RhlI and RhlR 3D Models

The focus of this study was on the *P. aeruginosa* proteins LasI, LasR, RhlI, RhlR, PqsA, and PqsR. The secondary structures of LasI, LasR, PqsA, and PqsR are available in the Protein Data Bank (PDB). However, the 3D structures of RhlI and RhlR are not available. Therefore, RhlI and RhlR were modeled to facilitate further analysis.

For the 3D model of RhlI, the QMEAN score was − 1.55 and the Global Model Quality Estimation (GMQE) score was 0.93. Ramachandran plot analysis performed using MolProbity v4.4 showed that 96.48% of the residues were in the allowed region, and 0% of the

residues were rotamers (Fig. 2a). Furthermore, none of the 1630 bonds in the model showed discordance in the MolProbity analysis. Similarly, for RhlR, the QMEAN score was − 0.31, and the GMQE score was 0.85. The Ramachandran plot revealed that 97% of the residues were in the allowed region, while 0.73% of the residues were rotamers, specifically Ser 182B, Met 18B, and Met 18A. Additionally, Asn 129A and Asn 129B were identified as Ramachandran outliers, constituting 0.43% of the residues (Fig. 2b). None of the 3890 bonds in the RhlR model showed discordance according to MolProbity analysis. The cumulative MolProbity score was 0.85 for RhlI and 1.21 for RhlR. These results demonstrated that the quality of the constructed models was consistent with published parameters for homology modeling [55, 56].

3.2 Assessment of Target Protein Interactions with AgNPs, ZnONPs, and CuONPs

Metal and metal oxide nanoparticles, such as silver, zinc oxide, and copper oxide, offer effective alternatives to conventional antibiotics, especially in the context of antibiotic resistance [28, 57]. These nanoparticles operate through distinct mechanisms, including quorum sensing inhibition, to combat resistant bacteria [58]. Their varied interactions with biomolecules further reduce the likelihood of new resistant strains, making them strong candidates for addressing antibiotic resistance [59].

Computational molecular docking studies have become essential for revealing the mechanisms underlying the antibacterial effects of nanoparticles and for advancing our understanding of their interactions with biological targets [60]. Targeting the QS system of pathogens like *P. aeruginosa* presents a significant opportunity to combat

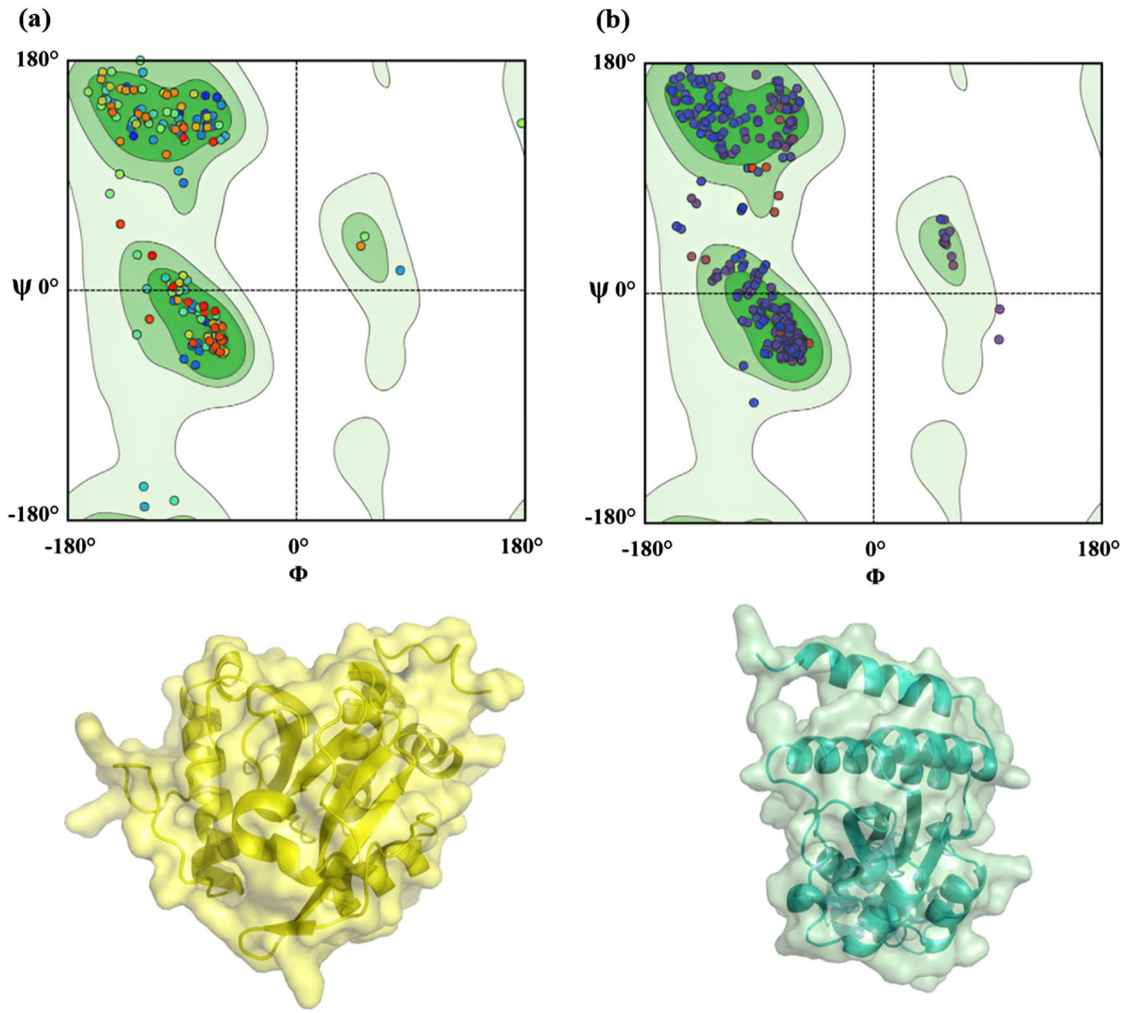

Fig. 2 Ramachandran plots for **a** RhlI and **b** RhlR from SWISS-MODEL, illustrating angles in favored, allowed, and unfavored regions. The plots show that 96.48% of RhlI residues and 97% of RhlR residues are in the allowed regions, with RhlR having 0.73% rotamers and specific outliers (Ser 182B, Met 18B, and Met 18A)

drug-resistant microbes. In this study, we concentrated on the LasI/R, RhlI/R, and PqsA/R systems, which are established targets of QS. Our molecular docking simulations provided insights into the binding affinities and inhibitory mechanisms of AgNPs, ZnONPs, and CuONPs against these QS proteins.

AutoDockTools was used for molecular docking, revealing that AgNPs, CuONPs, and ZnONPs successfully docked into AHL synthases LasI and RhlI, as well as regulatory activator proteins LasR and RhlR, and the transcriptional proteins PqsA and PqsR. The docked structures were visualized using Discovery Studio and PyMol, showing that the metallic nanoparticles were "locked" into the active sites of the specific QS proteins through interactions with the surrounding amino acid residues. Detailed data, including hydrogen bonds, hydrophobic bonds, binding energies, and predicted inhibition constants (Ki), are presented in Table 1. The QS receptor proteins LasR, RhlR, and PqsR, in conjunction with their respective natural signaling molecules (3-oxo-C12-HSL, C4-HSL, and PQS), regulate the expression of virulence factors, biofilm formation, bacterial motility, and other processes in *P. aeruginosa* [61]. However, competitive ligands with higher binding affinities to these receptors can inhibit these natural signaling molecules, potentially reducing QS-dependent factor formation.

To further investigate these interactions, we used the PrankWeb server to predict potential binding sites in each QS protein, confirming that the active site residues are identical to those reported in the literature [45, 47, 48]. Table 1 and Figs. 3, 4, 5, 6, 7, and 8 provide detailed information on binding energies, inhibition constants, and active amino acids for the metal and metal oxide nanoparticles. These findings enhance our understanding of the interactions between metal and metal oxide nanoparticles and bacterial QS systems, offering valuable insights into their potential applications as anti-QS and anti-biofilm age nts.

LasI is a homoserine lactone (HSL) synthesis protein in *P. aeruginosa* that catalyzes the production of 3-oxo-C12-HSL. It shares significant sequence similarity with RhlI, another AHL synthase in *P. aeruginosa*, indicating potential functional parallels [62]. In our molecular docking analysis, we investigated the interactions of Ag, ZnO, and CuO nanoparticles with the LasI protein (Fig. 3). AgNPs were observed to engage with the amino acid Met 54 of LasI via electrostatic interactions, producing an interaction energy of − 0.21 kcal/mol. In contrast, ZnONPs demonstrated hydrogen bonding with Ala175 and Glu163, alongside hydrophobic interactions with His89, Phe162, Gly163, and Ala175 within the LasI active site, resulting in a binding energy of − 2.72 kcal/mol. Similarly, CuONPs exhibited a binding energy of − 1.85 kcal/mol, forming five hydrogen bonds with Leu87, Phe162, Gly163, Pro164 and Ala175 within the LasI active site.

Table 1 Molecular docking results for metal and metal oxide nanoparticles and their interactions with quorum sensing proteins of *P. aeruginosa*

Protein name	Ligand	H-bond	Hydrophobic bond	Binding energy (kcal/mol)	Ki (mM)
LasI	Ag	–	Met 54	− 0.21	696.14
	ZnO	Gly163 – Ala 175	His 89—Phe 162 – Gly163 – Ala 175	− 2.72	10.09
	CuO	Leu 87 – Phe 162 – Gly 163 – Pro 164 – Ala 175	–	− 1.85	44.09
LasR	Ag	–	Tyr 56 – Lys 34	− 0.15	770.33
	ZnO	Asp 65 – Ala 70	Glu 48 – Asp 65 – Ala 70	− 2.58	12.86
	CuO	Tyr 64—Asp 65– Tyr 69—Ala 70	–	− 1.63	63.85
RhlI	Ag	–	Arg 71 – Glu 101 – Ser 103	− 0.19	720.04
	ZnO	Leu 88 – Gly 158 – Pro 159 – Ala 170	Leu 88 – Gly 158 –Ala 170	− 2.47	15.37
	CuO	Leu 88 – Gly 158 – Leu 168—Ala 170	–	− 1.68	58.72
RhlR	Ag	–	Tyr 43 – Tyr 64	− 0.15	778.18
	ZnO	Tyr 64	Tyr 64	− 2.51	14.43
	CuO	Tyr 43 – Tyr 64	–	− 1.57	70.25
PqsA	Ag	–	Gly 173 – Trp 363 –Arg 364	− 0.22	686.89
	ZnO	Gly 173 – Trp 363 – Arg 364	Asp 98 – Gly 173 – Trp 363 – Arg 364	− 3.83	1.65
	CuO	Gly 173 – Trp 363 – Arg 364	Asp 98	− 2.49	15.00
PqsR	Ag	–	Ile 147 – Thr 148	− 0.19	729.83
	ZnO	Gln 194 – Ile 195 – Ser 196 – Ile 236	Gln 194 – Ile 195 – Ser 196 – Trp 234 – Ile 236	− 2.86	8.08
	CuO	Gln 194 – Ile 195 – Ile 236	–	− 1.93	38.59

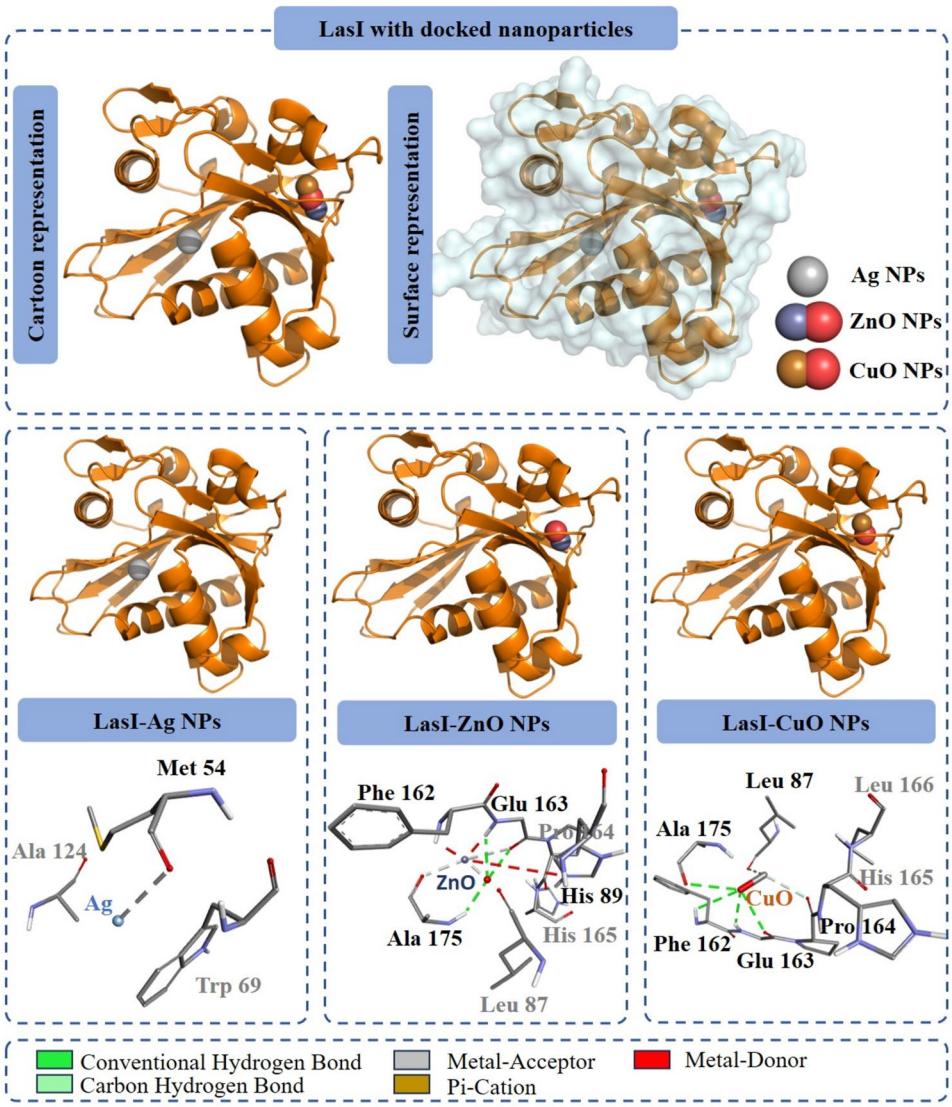

Fig. 3 Interaction profiles of LasI with AgNPs, ZnONPs, and CuONPs; green dashed lines indicate hydrogen bonds, while gray and red dashed lines represent electrostatic bonds

Our in silico docking analysis indicates that Ag, ZnO, and CuO nanoparticles may form complexes with the LasI protein, potentially competing with its native ligand, S-adenosyl-L-methionine (SAM). This interaction could inhibit the activation of quorum sensing-regulated proteins such as LasR, RhlR, RhlI, PqsA, and PqsR, thereby disrupting quorum sensing signaling pathways. In addition to assessing the binding energies, we evaluated the inhibition constants (Ki) of AgNPs, ZnONPs, and CuONPs with the LasI protein, to further elucidate their affinity. Interestingly, the Ki value for the LasI-ZnONPs complex (10.09 mM) was lower than those for the LasI-AgNPs (696.14 mM) and LasI-CuONPs (44.09 mM) complexes. This suggests that ZnO nanoparticles exhibit a higher affinity for the LasI protein compared to AgNPs and CuONPs. Furthermore, our investigation extended to analyzing the binding energy of the LasI-ZnONPs complex, providing insights into the stability of this nanoparticle-protein interaction. Notably, the binding energy of the LasI-ZnONPs complex (− 2.72 kcal/mol) was significantly higher than that of well-known quorum sensing inhibitors (QSIs) such as furanone C30 (− 2.39 kcal/mol) and the natural ligand gingerol (− 2.55 kcal/mol), as reported in seminal scientific studies [63, 64]. This pivotal finding strongly suggests that ZnO nanoparticles have the potential to inhibit AHL production, a critical step in disrupting quorum sensing mechanisms.

LasR, a key transcriptional activator regulating the expression of virulence-related genes in *P. aeruginosa*, is a crucial target for therapeutic interventions [65]. Notably, the Las system serves as the principal regulator of QS in *P. aeruginosa*, controlling both the Rhl and Pqs signaling pathways [66]. Our molecular docking analysis revealed that AgNPs interact with the LasR protein with a binding energy of − 0.15 kcal/mol, primarily involving the amino acid residues Tyr 56 and Lys 34 (Fig. 4). These residues overlap

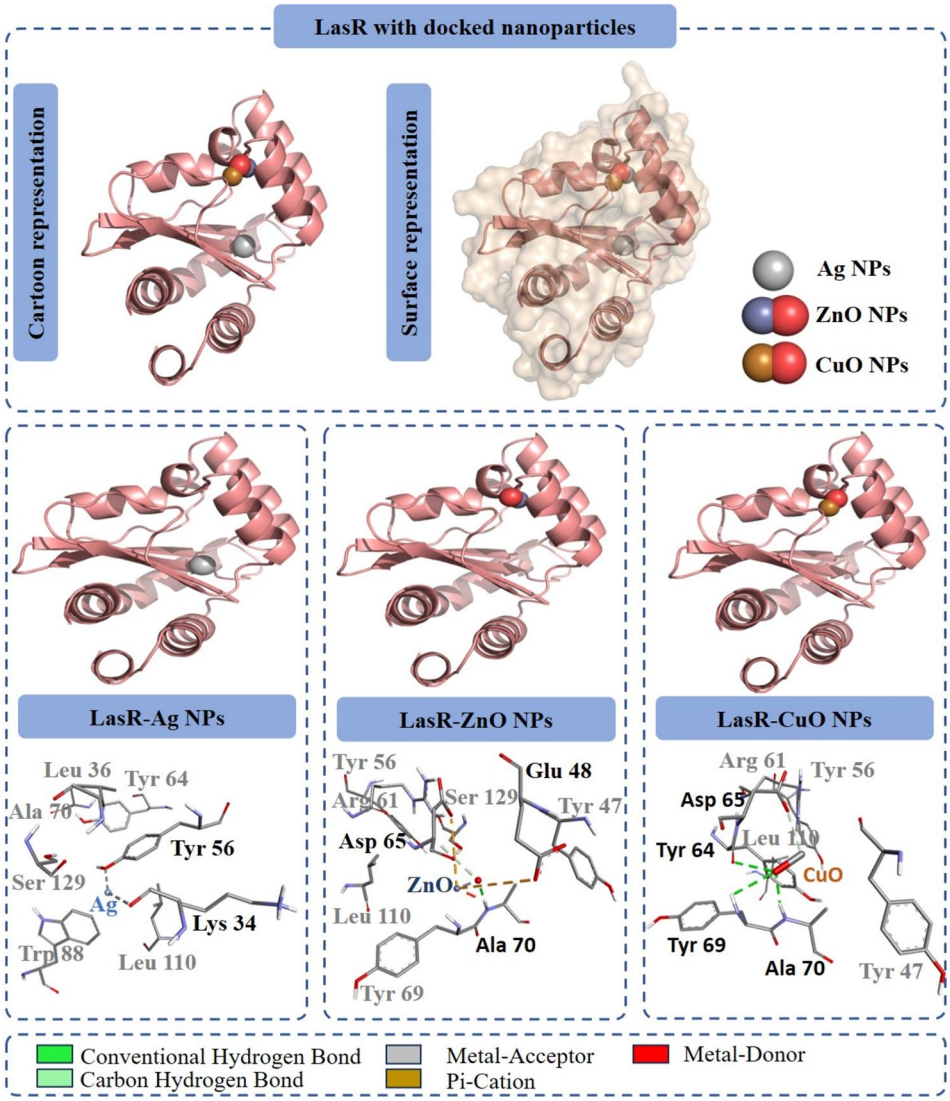

Fig. 4 Interaction profiles of LasR with AgNPs, ZnONPs, and CuONPs as predicted by AutoDockTools; green dashed lines indicate hydrogen bonds, while gray and red dashed lines represent electrostatic bonds

with known binding sites of LasR inhibitors, indicating a potential competitive mechanism for AgNPs [67].

Further docking analysis revealed that ZnONPs bind to LasR with a binding energy of − 2.58 kcal/mol, interacting with key residues Glu48, Asp65, and Ala70, stabilized by hydrogen bonds with Asp65 and Ala70. Similarly, CuONPs exhibited a binding energy of − 1.63 kcal/mol, with interactions primarily stabilized by hydrogen bonds involving Tyr64, Asp65, Tyr69, and Ala70. These results suggest that Ag, CuO, and ZnO nanoparticles may compete with the native ligand 3-O-C12-HSL, thereby downregulating LasR-mediated virulence factor production [68].

To further evaluate the inhibitory potential of these nanoparticles, we determined their inhibitory constant (Ki) against LasR. The results indicated that the LasR-ZnONPs complex had a significantly lower Ki value (12.86 mM) compared with the LasR-AgNPs (770.33 mM) and LasR-CuONPs (63.85 mM), highlighting the stronger binding affinity of ZnONPs to LasR protein. ZnONPs interacted with Ala70 in the same binding cavity where the natural ligand 3-oxo-C12-HSL binds [69, 70], further supporting the conclusion that ZnONPs are the most effective among the tested nanoparticles. Since the binding of 3-oxo-C12-HSL to LasR triggers the transcription of various virulence genes in *P. aeruginosa* [71], it is anticipated that ZnONPs could compete with 3-oxo-C12-HSL for binding to LasR, thereby reducing the expression of QS-controlled genes.

RhlI, the synthase responsible for producing the quorum sensing molecule N-butyryl-L-homoserine lactone (C4-HSL), plays a pivotal role in regulating *P. aeruginosa* pathogenicity by binding to its receptor RhlR, as reported by Kumar et al. [48]. Our docking studies revealed that RhlI binds with AgNPs, exhibiting a binding energy of − 0.19 kcal/mol, with key interacting residues including Arg71, Glu101, and Ser103. Docking analysis of RhlI with CuONPs revealed a binding energy of − 1.68 kcal/

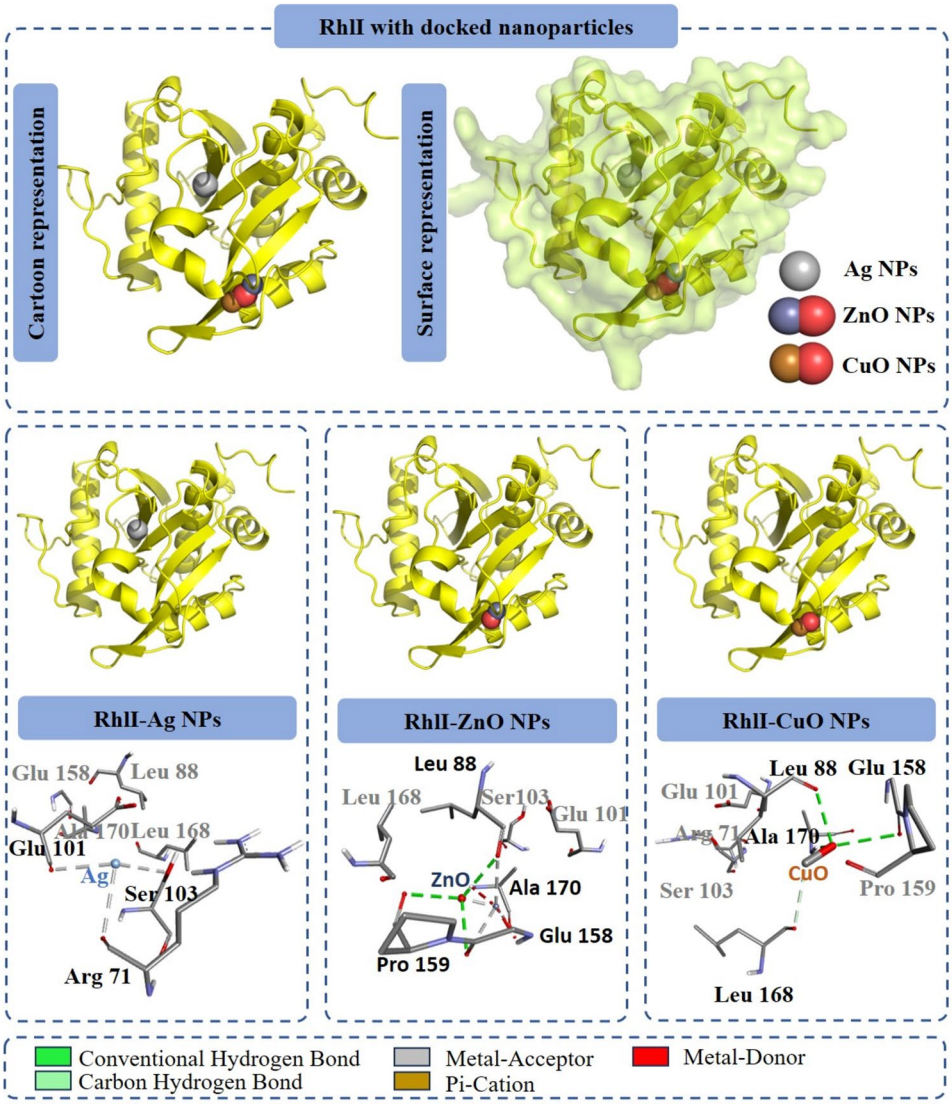

Fig. 5 Interaction profiles of RhlI with AgNPs, ZnONPs, and CuONPs as predicted by AutoDockTools; green dashed lines indicate hydrogen bonds, while gray and red dashed lines represent electrostatic bonds

mol, supported by hydrogen bonds involving Leu88, Gly158, Leu168, and Ala170. In contrast, the docking of RhlI with ZnONPs exhibited a significantly stronger binding energy of − 2.47 kcal/mol, involving interaction with Leu88, Gly158, Pro159, and Ala170, with hydrogen bonds stabilizing the complex at Gly158, Pro159, and Ala170 (Fig. 5). Additionally, the Ki value for the RhlI-ZnONPs complex (15.37 mM) was significantly lower than those for the RhlI-AgNPs (720.04 mM) and RhlI-CuONPs (58.72 mM) complexes (Table 1). This stronger binding and lower Ki value suggest that ZnO nanoparticles have a higher potential to interfere with RhlI function, possibly disrupting quorum sensing and reducing *P. aeruginosa* pathogenicity. In line with our findings, Saleh et al. demonstrated that ZnO nanoparticles significantly reduce the expression levels of the QS regulatory gene RhlI [72]. Moreover, our work highlights the importance of direct interactions between nanoparticles and QS proteins, which can lead to changes in their activity and subsequent effects on QS signaling pathways.

RhlR, the receptor for the AHL produced by the RhlI synthase, plays a crucial role in activating virulence genes in *P. aeruginosa* [73]. Upon binding with C4-HSL, RhlR triggers the transcription of numerous virulence genes [74–77]. Our docking studies of RhlR with AgNPs, ZnONPs, and CuONPs revealed distinct interaction patterns and binding affinities (Fig. 6). The RhlR-AgNPs complex formed two electrostatic interactions with Tyr43 and Tyr64, resulting in a binding energy of − 0.15 kcal/mol. In contrast, the RhlR-CuONPs complex exhibited a binding energy of − 1.68 kcal/mol, stabilized primarily by hydrogen bonds involving Tyr43 and Tyr64. Notably, the RhlR-ZnONPs complex showed the highest binding affinity with a binding energy of − 2.51 kcal/mol, supported by a hydrogen bond with Tyr64.

Interestingly, all three nanoparticles, AgNPs, ZnONPs, and CuONPs were docked at Tyr64, which is located within

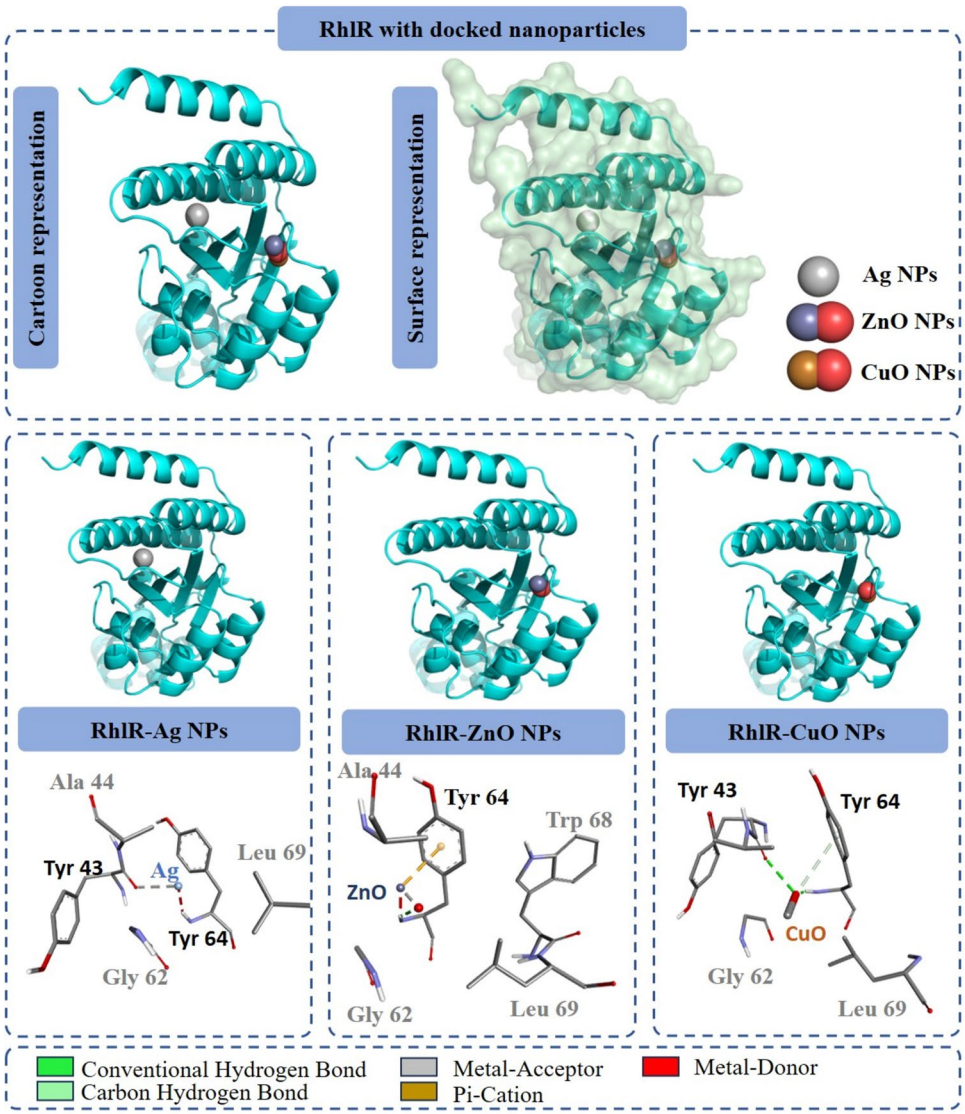

Fig. 6 Interaction profiles of RhlR with AgNPs, ZnONPs, and CuONPs as predicted by AutoDockTools; green dashed lines indicate hydrogen bonds, while gray and red dashed lines represent electrostatic bonds

the same binding cavity where RhlR's, natural ligand, C4-HSL, binds, as previously reported [70, 78, 79]. This observation aligns with the crystallographic findings of Borgert et al. (2022), which demonstrated that C4-HSL interacts with the active site of RhlR, forming hydrogen bonds with Tyr64 [78]. Our docking studies suggest that ZnONPs, AgNPs, and CuONPs can occupy this critical site, potentially competing with C4-HSL for binding to RhlR. The binding potential of ZnONPs to RhlR was higher compared with AgNPs and CuONPs, as indicated by a significantly lower Ki value for the RhlR-ZnONPs complex (14.43 mM) compared with the RhlR-AgNPs (778.18 mM) and RhlR-CuONPs (70.25 mM) complexes (Table 1). This suggests that ZnONPs may more effectively compete with C4-HSL for binding to RhlR, potentially interfering with quorum sensing at the protein level. These findings highlight the varying binding affinities and interaction mechanisms between RhlR and different nanoparticles, with ZnONPs demonstrating the strongest interaction and thus presenting potential as modulators of quorum sensing pathways.

In addition to the Las/Rhl system, the **PQS** (Pseudomonas quinolone signal) system is another key crucial quorum sensing system pathway in *P. aeruginosa* that play a significant role in biofilm formation. Disrupting this system can be effective for controlling biofilm-related infections [80]. **PqsA** is a crucial enzyme involved in the production of PQS signaling molecules [81, 82], making it a promising target for developing therapies against multidrug-resistant *P. aeruginosa* [83].

Our molecular docking studies revealed that AgNPs interact with the amino acids Gly173, Trp363, and Arg364 of PqsA through electrostatic interactions, with a binding energy of − 0.22 kcal/mol (Table 1). In contrast, the PqsA-ZnO nanoparticle complex showed a much stronger

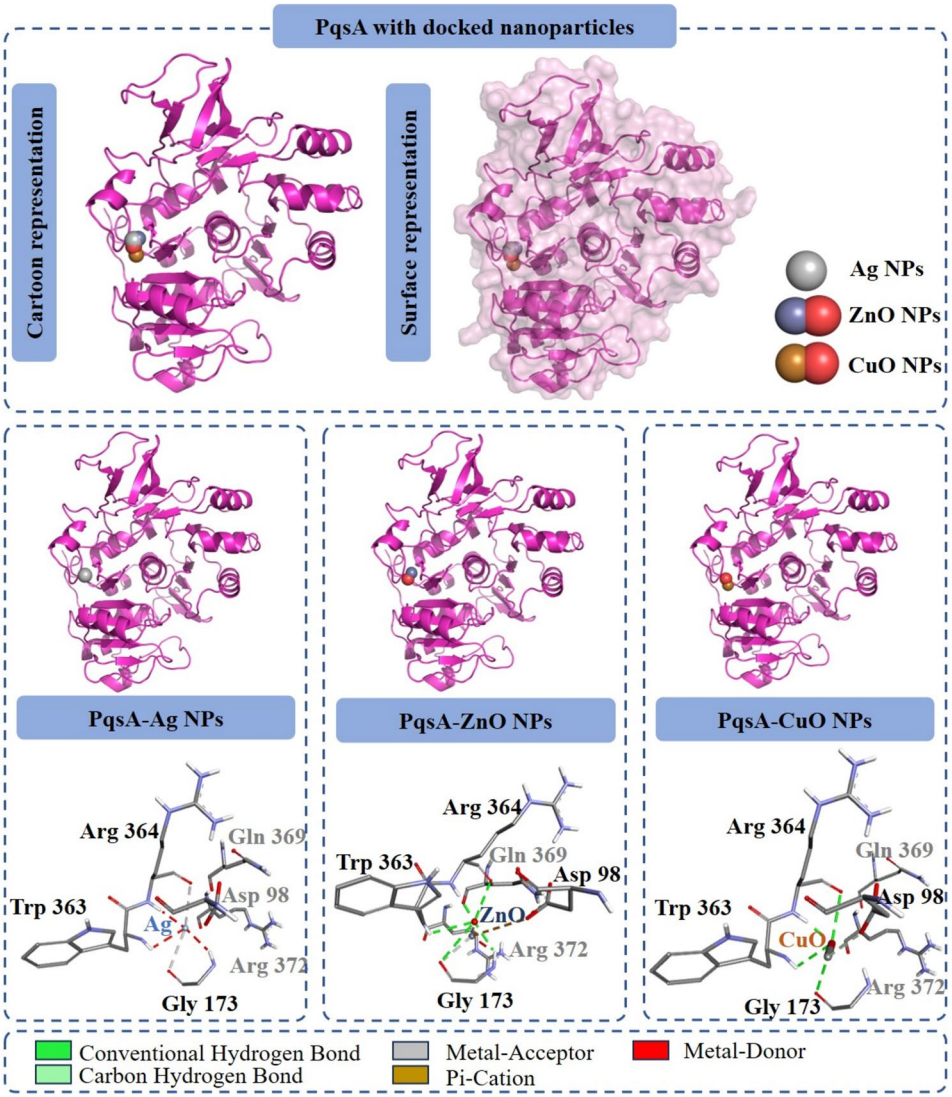

Fig. 7 Interaction profiles of PqsA with AgNPs, ZnONPs, and CuONPs as predicted by AutoDockTools; green dashed lines indicate hydrogen bonds, while gray and red dashed lines represent electrostatic bonds

binding energy of − 3.83 kcal/mol, stabilized through hydrogen bonds involving Gly173, Trp363, and Arg364, as well as hydrophobic interactions with Asp98, Gly173, Trp363, and Arg364 at the active site of PqsA. Similarly, docking of PqsA with CuONPs resulted in binding energy of − 2.49 kcal/mol, with interactions stabilized by hydrogen bonds involving key residues Asp98, Gly173, Trp363, and Arg364 and additional hydrophobic interaction with Asp98 (Fig. 7).

The PqsA-ZnONPs complex exhibited the highest affinity among the tested nanoparticles, with a significantly lower Ki value (1.65 mM) compared with the PqsA-AgNPs (686.89 mM) and PqsA-CuONPs (15.00 mM) complexes (Table 1). This finding aligns with the study by M. Saleh et al. [72], which reported that ZnO nanoparticles reduce the expression of the *pqsA* gene at the transcriptional level before the PqsA protein is produced. However, our study highlights a complementary mechanism: We show that ZnONPs can directly bind to the PqsA protein, potentially inhibiting its function at the protein level. This distinction is important because while gene expression changes reduce the amount of PqsA produced, our results suggest that ZnONPs can also impair the activity of any PqsA that is already present. Since PqsA is critical for PQS signaling molecule production, targeting it at both the gene and protein levels could enhance strategies to disrupt PqsR-dependent gene regulation and biofilm formation in *P. aeruginosa* [81, 82].

PqsR, a key transcriptional regulator in *P. aeruginosa*, plays a crucial role in controlling the expression of virulence genes. It becomes activated upon binding to 2-heptyl-4-quinolone (HHQ) and the Pseudomonas quinolone signal (PQS) [84]. PqsR regulates the polycistronic operon pqsABCDE, which contains essential genes for encoding the synthases involved in PQS and HHQ production [85].

Our docking studies demonstrate that PqsR interacts with AgNPs through two electrostatic bonds with the

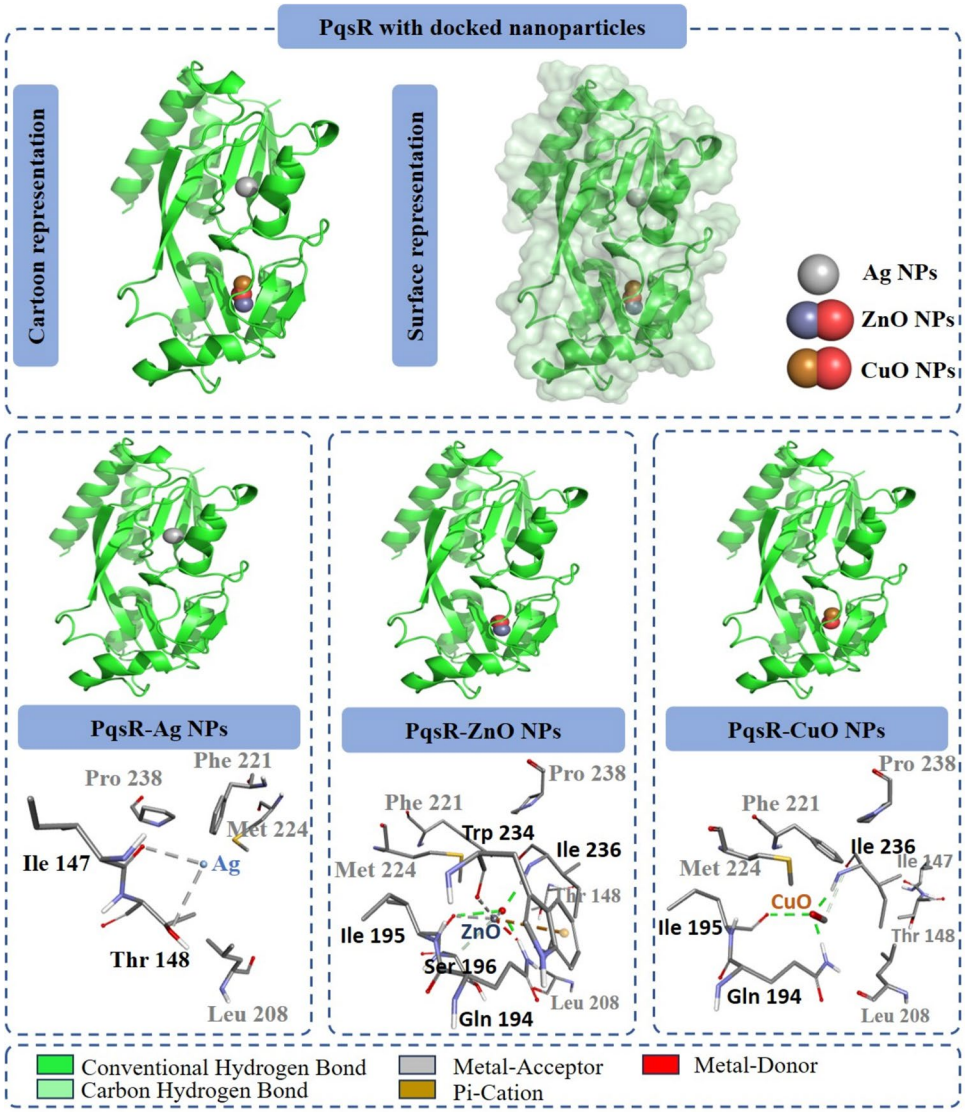

Fig. 8 Interaction profiles of PqsR with AgNPs, ZnONPs, and CuONPs as predicted by AutoDockTools; green dashed lines indicate hydrogen bonds, while gray and red dashed lines represent electrostatic bonds

Ile147 and Thr148 (Fig. 8), resulting in a binding energy of − 0.19 kcal/mol. In contrast, ZnONPs showed a significantly stronger interaction with PqsR, with a binding energy of − 2.86 kcal/mol, stabilized by hydrogen and hydrophobic bonds involving Gln194, Ile195, Ser196, Trp234, and Ile236. The PqsR-CuONPs complex exhibited a binding energy of − 1.93 kcal/mol, stabilized by hydrogen bonds with Gln194, Ile195, and Ile236.

ZnONPs displayed a superior binding affinity to PqsR compared with AgNPs and CuONPs, with a notably lower Ki (8.08 mM) than the PqsR-AgNPs (729.83 mM) and PqsR-CuONPs (38.59 mM) complexes (Table 1). ZnONPs occupy the binding region of the co-crystallized ligand 3NH2-7Cl-C9QZN in PqsR, interacting with key amino acid residues Gln196, Ser236, and Ile236. These findings suggest that ZnONPs could competitively inhibit PqsR activation in *P. aeruginosa* by occupying the same binding pocket as other ligands [45].

Our study reveals the interactions between metal and metal oxide nanoparticles and the QS systems of *P. aeruginosa*, identifying ZnONPs as the most effective inhibitors. In *P. aeruginosa*, amino acids such as arginine, ornithine, isoleucine, leucine, valine, phenylalanine, and tyrosine enhance biofilm formation while reducing swarming motility [86]. Additionally, Other studies have highlighted the role of aspartic acid, histidine, leucine, methionine, tryptophan, and tyrosine in biofilm assembly [87]. Our findings further show that ZnONPs interact with key amino acid residues, such as aspartic acid, tryptophan, and arginine (Table 1), within the active sites of QS signaling proteins.

Molecular docking results indicate that ZnONPs form strong hydrogen and hydrophobic bonds with the key QS

proteins LasI, LasR, RhlI, RhlR, PqsA, and PqsR, with binding energies ranging from − 2.47 to − 3.83 kcal/mol, outperforming AgNPs and CuONPs. The location of AgNPs within the active sites differs slightly from that of ZnONPs and CuONPs. This difference arises from the molecular characteristics of each nanoparticle. AgNPs, being metallic, primarily interact with proteins through hydrophobic contacts, favoring non-polar regions. In contrast, ZnONPs and CuONPs, as metal oxides, engage more through hydrogen bonds and polar interactions, promoting interactions with charged and polar residues. This distinction significantly influences the type and location of attachment to each protein.

This strong binding affinity suggests that ZnONPs can effectively inhibit the synthesis of QS signaling molecules by binding to acyl-homoserine-lactone synthases (LasI, RhlI, PqsA) and disrupt their binding to regulatory proteins (LasR, RhlR, PqsR). This competitive binding mechanism impedes the normal signaling processes within *P. aeruginosa*, leading to a reduction in its pathogenicity. Analysis of protein–ligand interactions suggests that ligands with high efficiency are generally enriched with hydrophobic interactions [88], which may contribute to their enhanced stability and inhibitory potential [89].

ZnONPs exhibited superior binding affinities, as evidenced by their lower inhibition constants, compared with AgNPs and CuONPs. This suggests that ZnONPs can effectively compete with native ligands-such as S-adenosyl-L-methionine, 3O-C12-HSL, C4-HSL, and PQS-disrupting QS signaling pathways. Notably, to our knowledge, this is the first in silico investigation of the interaction between ZnONPs and PqsA and PqsR proteins (Table 1).

Our docking studies revealed that ZnONPs showed the strongest affinity for PqsA, with a binding energy of − 3.83 kcal/mol, compared with CuONPs and AgNPs. This indicates that ZnONPs might effectively block the binding pocket of PqsA, potentially inhibiting the entry of natural ligands and, thus, its activation. Previous research has shown that the pqs system plays a crucial role in regulating pyocyanin production, suggesting that ZnONPs could interfere with this process. Furthermore, the lower Ki for the PqsA-ZnONPs complex suggests greater stability compared to other nanoparticle complexes.

Interestingly, ZnONPs do not share structural similarities with traditional AHLs and SAM molecules involved in QS, presenting a novel method for inhibiting QS-controlled genes and offering a potential treatment for *P. aeruginosa* infections. Additionally, due to their smaller size and high surface area-to-volume ratio, nanoparticles like ZnONPs are particularly effective in penetrating microbial cells and enhancing drug delivery [90]. The stability and favorable binding profile of the PqsA-ZnONPs complex were further supported by molecular dynamics simulations.

3.3 Dynamic Simulation Studies

Molecular dynamics (MD) simulation is crucial for assessing the stability of the receptor-ligand complex [91]. In this study, the protein analyzed is the cell communication protein PqsA from *P. aeruginosa*, represented by the crystalline structure with the PDB code 5OE3. The PqsA protein showed strong interaction energies with silver, zinc oxide, and copper oxide nanoparticles. The simulation specifically focused on the PqsA-ZnONPs complex, revealing it to be the most stable among the three types of nanoparticles studied. The stability of the protein structure and structural changes were monitored by calculating the RMSD during the simulation.

After an initial adjustment period of the ligand within the protein cavity, the RMSD of the ZnONPs remained stable, ranging from 2.5 to 4 Å throughout the simulation. Figure 9a illustrates the RMSD profiles of the complex formed by the PqsA protein from *P. aeruginosa* and ZnONPs, showing a slight variation but consistent stability over time. The nanoparticle underwent more fluctuations due to the large active site cavity, with fluctuations between 3 and 4 Å.

The movement of amino acids within the active site was assessed by calculating the RMSF of the macromolecule's Cα atoms, which characterize the fluctuations of amino acids relative to their initial positions. The RMSF values for residues are plotted on the y-axis, with residue numbers displayed on the x-axis. The majority of residues in the macromolecular backbone exhibited RMSF values ranging from 0.5 to 2.5 Å, which is considered acceptable for residues within an active site. The ZnONPs might be interacting with PqsA in more flexible regions, allowing them to adapt their shapes to each other. It is important to note that the highest RMSF value corresponds to a greater degree of movement, while the lowest RMSF value indicates a more stable structure with limited structural fluctuations during the MD simulation [92, 93]. The RMSF plot for the Cα backbones of the receptor macromolecule generated by the 100 ns MD simulation is shown in Fig. 9d.

During the simulation process, a significant portion of the macromolecular secondary structures (42.11%) were conserved, with α-helices comprising 22.78% and β-sheets comprising 19.33%. Throughout the MD simulation, the stability of the receptor-ligand complex was upheld by the presence of hydrogen bonds, hydrophobic contacts, and ionic interactions. ZnONPs were found to interact with specific amino acid residues of the quorum sensing protein of *P. aeruginosa*, including Trp363, Arg364, and Gln369 via hydrogen bonds, and Asp98, Pro171, Gly173, and Ser366 via water bridges. The details of the interactions observed between ZnONPs and the PqsA protein of *P. aeruginosa* are demonstrated in Fig. 9b.

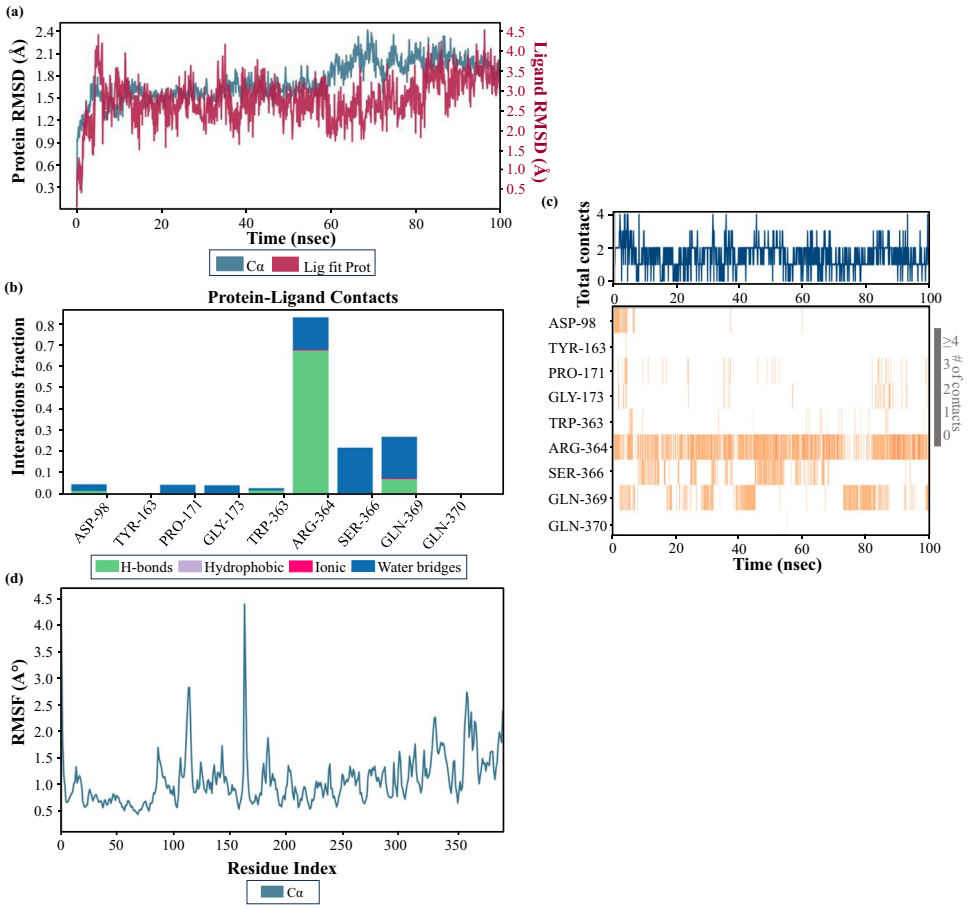

Fig. 9 Analysis of ligand–protein interactions over simulation time. **a** Root-mean-square deviations (RMSD) for backbone atoms and ligands. **b** Protein–ligand interaction profile for PqsA in complex with ZnONPs. **c** Timeline representation of ligand–protein contacts: the top panel shows the total number of contacts, while the heat map depicts the interacting amino acid residues. **d** Root-mean-square fluctuation (RMSF) calculations of protein–ligand complexes throughout the 100 ns simulation

The dominant interaction is hydrophobic, suggesting the protein and ZnONPs bind through nonpolar forces. Hydrogen bonding is also observed to a lesser extent, with few ionic interactions and water bridges between the protein and nanoparticle. Figure 9c illustrates the timeline evolution of ligand–protein contacts during the 100 ns simulation period. The intensity of the band color positively correlates with the number of mediated contacts. Arg364 consistently exhibits the highest number of contacts, suggesting its significant role in the stability and interactions within the system. The results of the molecular dynamics simulation validate the results obtained by molecular docking, indicating that ZnONPs are stabilized by Asp98, Gly173, Trp363, and Arg364 (Table 1).

3.4 Conclusions

In this study, we demonstrated the anti-QS activity of metal and metal oxide nanoparticles, focusing on their molecular mechanisms against the superbug *P. aeruginos*a. Docking results showed that ZnONPs consistently bind to the active sites of QS regulators LasI/R, RhlI/R, and PqsA/PqsR, indicating their potential as antivirulence agents targeting QS signaling in *P. aeruginosa*. Specifically, the PqsA-ZnONPs complex exhibited strong predicted binding affinities, suggesting a significant role in disrupting the QS system in *P. aeruginosa*. Molecular dynamic simulations confirmed the stability of ZnONPs binding to the PqsA active site. The potential mechanisms of their anti-QS activity may include the inhibition of signal molecule synthesis and the blockage of receptor proteins. These findings highlight the promising potential of ZnONPs as effective inhibitors of virulence factors in Gram-negative bacteria, paving the way for their development as powerful agents against QS and biofilm formation.

Supplementary Information The online version contains supplementary material available at https://doi.org/10.1007/s12668-024-01625-4.

Acknowledgements The authors would like to thank the CNRST (National Center for Scientific and Technical Research) of Morocco and the Ministry of Higher Education in Morocco for their valuable support of this work.

Author Contribution All authors contributed equally to writing and reviewing the manuscript.

Funding None

Data Availability No datasets were generated or analysed during the current study.

Declarations

Ethics Approval This study did not involve human or animal subjects, so no ethical considerations or informed consent apply.

Consent to Participate Not applicable.

Consent for Publication Not applicable.

Conflict of Interest The authors declare no competing interests.

Research Involving Humans and Animals Statement None.

Informed Consent None.

References

1. Sadikot, R. T., Blackwell, T. S., Christman, J. W., & Prince, A. S. (2005). Pathogen-host interactions in pseudomonas aeruginosa pneumonia. *American Journal of Respiratory and Critical Care Medicine, 171*(11), 1209–1223. https://doi.org/10.1164/rccm.200408-1044SO
2. Qin, S., Xiao, W., Zhou, C., Pu, Q., Deng, X., Lan, L., Liang, H., Song, X., & Wu, M. (2022). Pseudomonas aeruginosa: Pathogenesis, virulence factors, antibiotic resistance, interaction with host, technology advances and emerging therapeutics. *Signal Transduction and Targeted Therapy, 7*(1), 199. https://doi.org/10.1038/s41392-022-01056-1
3. Osmon, S., Ward, S., Fraser, V. J., & Kollef, M. H. (2004). Hospital mortality for patients with bacteremia due to Staphylococcus aureus or Pseudomonas aeruginosa. *Chest, 125*(2), 607–616. https://doi.org/10.1378/chest.125.2.607
4. Chadha, J., Harjai, K., & Chhibber, S. (2022). Repurposing phytochemicals as anti-virulent agents to attenuate quorum sensing-regulated virulence factors and biofilm formation in Pseudomonas aeruginosa. *Microbial Biotechnology, 15*(6), 1695–1718. https://doi.org/10.1111/1751-7915.13981
5. Rashiya, N., Padmini, N., Ajilda, A. A. K., Prabakaran, P., Durgadevi, R., Ravi, A. V., Ghosh, S., Sivakumar, N., & Selvakumar, G. (2021). Inhibition of biofilm formation and quorum sensing mediated virulence in Pseudomonas aeruginosa by marine sponge symbiont Brevibacterium casei strain Alu 1. *Microbial Pathogenesis, 150*, 104693. https://doi.org/10.1016/j.micpath.2020.104693
6. Davies, D. G., Parsek, M. R., Pearson, J. P., Iglewski, B. H., Costerton, J. W., & Greenberg, E. P. (1998). The involvement of cell-to-cell signals in the development of a bacterial biofilm. *Science, 280*(5361), 295–298. https://doi.org/10.1126/science.280.5361.295
7. Lewis, K. (2001). Riddle of biofilm resistance. *Antimicrobial Agents and Chemotherapy, 45*(4), 999–1007. https://doi.org/10.1128/AAC.45.4.999-1007.2001
8. Rollet, C., Gal, L., & Guzzo, J. (2009). Biofilm-detached cells, a transition from a sessile to a planktonic phenotype: A comparative study of adhesion and physiological characteristics in pseudomonas aeruginosa. *FEMS Microbiology Letters, 290*(2), 135–142. https://doi.org/10.1111/j.1574-6968.2008.01415.x
9. Liu, J., Zhao, S. Y., Hu, J. Y., Chen, Q. X., Jiao, S. M., Xiao, H. C., Zhang, Q., Xu, J., Zhao, J. F., Zhou, H. B., et al. (2023). Novel coumarin derivatives inhibit the quorum sensing system and iron homeostasis as antibacterial synergists against Pseudomonas aeruginosa. *Journal of Medicinal Chemistry, 66*(21), 14735–14754. https://doi.org/10.1021/acs.jmedchem.3c01268
10. Kar, A., Mukherjee, S. K., Barik, S., & Hossain, S. T. (2024). Antimicrobial activity of trigonelline hydrochloride against Pseudomonas aeruginosa and its quorum-sensing regulated molecular mechanisms on biofilm formation and virulence. *ACS Infectious Diseases, 10*(2), 746–762. https://doi.org/10.1021/acsinfecdis.3c00617
11. Rutherford, S. T., & Bassler, B. L. (2012). Bacterial quorum sensing: Its role in virulence and possibilities for its control. *Cold Spring Harbor Perspectives in Medicine, 2*(11), a012427–a012427. https://doi.org/10.1101/cshperspect.a012427
12. Choi, H., Ham, S. Y., Cha, E., Shin, Y., Kim, H. S., Bang, J. K., Son, S. H., Park, H. D., & Byun, Y. (2017). Structure–activity relationships of 6- and 8-gingerol analogs as anti-biofilm agents. *Journal of Medicinal Chemistry, 60*(23), 9821–9837. https://doi.org/10.1021/acs.jmedchem.7b01426
13. El-Mowafy, S. A., Abd El Galil, K. H., El-Messery, S. M., & Shaaban, M. I. (2014). Aspirin is an efficient inhibitor of quorum sensing, virulence and toxins in Pseudomonas aeruginosa. *Microbial Pathogenesis, 74*, 25–32. https://doi.org/10.1016/j.micpath.2014.07.008
14. Bahari, S., Zeighami, H., Mirshahabi, H., Roudashti, S., & Haghi, F. (2017). Inhibition of Pseudomonas aeruginosa quorum sensing by subinhibitory concentrations of curcumin with gentamicin and azithromycin. *Journal of Global Antimicrobial Resistance, 10*, 21–28. https://doi.org/10.1016/j.jgar.2017.03.006
15. McKnight, S. L., Iglewski, B. H., & Pesci, E. C. (2000). The Pseudomonas quinolone signal regulates rhl quorum sensing in Pseudomonas aeruginosa. *Journal of Bacteriology, 182*(10), 2702–2708. https://doi.org/10.1128/JB.182.10.2702-2708.2000
16. Zhou JW, Li PL, Ji PC, Yin KY, Tan XJ, Chen H, Xing XD, Jia AQ. (2024). Carbon quantum dots derived from resveratrol enhances anti-virulence activity against Pseudomonas aeruginosa. *Surfaces and Interfaces*, *44*(August 2023), 103662. https://doi.org/10.1016/j.surfin.2023.103662
17. Wagener, B. M., Hu, R., Wu, S., Pittet, J. F., Ding, Q., & Che, P. (2021). The role of pseudomonas aeruginosa virulence factors in cytoskeletal dysregulation and lung barrier dysfunction. *Toxins*, *13*(11). https://doi.org/10.3390/toxins13110776
18. Xu, Q., Kang, D., Meyer, M. D., Pennington, C. L., Gopal, C., Schertzer, J. W., & Kirienko, N. V. (2024). Cytotoxic rhamnolipid micelles drive acute virulence in Pseudomonas aeruginosa. *Infection and Immunity*, *92*(3). https://doi.org/10.1128/iai.00407-23
19. Zhou, J. W., Ji, P. C., Wang, C. Y., Yang, Y. J., Zhao, X. Y., & Tang, H. Z. (2023). Anti-virulence activity of dihydrocuminyl aldehyde and nisin against spoilage bacterium Pseudomonas aeruginosa XZ01. *Lwt, 177*(February), 114573. https://doi.org/10.1016/j.lwt.2023.114573
20. Chen, H., Ji, P. C., Qi, Y. H., Chen, S. J., Wang, C. Y., Yang, Y. J., Zhao, X. Y., & Zhou, J. W. (2023). Inactivation of Pseudomonas aeruginosa biofilms by thymoquinone in combination with nisin. *Frontiers in Microbiology, 13*(January), 1–17. https://doi.org/10.3389/fmicb.2022.1029412
21. Alvarez, M. V., Moreira, M. R., & Ponce, A. (2012). Antiquorum sensing and antimicrobial activity of natural agents with potential use in food. *Journal of Food Safety, 32*(3), 379–387. https://doi.org/10.1111/j.1745-4565.2012.00390.x
22. Hurley, M. N., Cámara, M., & Smyth, A. R. (2012). Novel approaches to the treatment of Pseudomonas aeruginosa infections in cystic fibrosis. *European Respiratory Journal, 40*(4), 1014–1023. https://doi.org/10.1183/09031936.00042012
23. Kalia, V. C. (2013). Quorum sensing inhibitors: An overview. *Biotechnology Advances, 31*(2), 224–245. https://doi.org/10.1016/j.biotechadv.2012.10.004
24. Qu, Y., Zou, Y., Wang, G., Zhang, Y., & Yu, Q. (2024). Disruption of communication: Recent advances in antibiofilm materials with anti-quorum sensing properties. *ACS Applied Materials and*

Interfaces, 16(11), 13353–13383. https://doi.org/10.1021/acsami.4c01428
25. Juszczuk-Kubiak, E. (2024). Molecular aspects of the functioning of pathogenic bacteria biofilm based on quorum sensing (QS) signal-response system and innovative non-antibiotic strategies for their elimination. *International Journal of Molecular Sciences*, *25*(5). https://doi.org/10.3390/ijms25052655
26. de Celis, M., Belda, I., Marquina, D., & Santos, A. (2022). Phenotypic and transcriptional study of the antimicrobial activity of silver and zinc oxide nanoparticles on a wastewater biofilm-forming Pseudomonas aeruginosa strain. *Science of the Total Environment, 826*, 153915. https://doi.org/10.1016/j.scitotenv.2022.153915
27. Sadoq, B-E., Britel, M. R., Bouajaj, A., Maâlej, R., Touhami, A., Abid, M., Douiri, H., Touhami, F., Maurady, A. (2022). A review on antibacterial activity of nanoparticles, *13*(5), 405. https://doi.org/10.33263/BRIAC135.405
28. Alavi, M., Li, L., & Nokhodchi, A. (2023). Metal, metal oxide and polymeric nanoformulations for the inhibition of bacterial quorum sensing. *Drug Discovery Today, 28*(1), 1–11. https://doi.org/10.1016/j.drudis.2022.103392
29. Li, Z., Zhang, Y., Huang, D., Huang, L., Zhang, H., Li, N., & Wang, M. (2021). Through quorum sensing, Pseudomonas aeruginosa resists noble metal-based nanomaterials toxicity. *Environmental Pollution*, *269*. https://doi.org/10.1016/j.envpol.2020.116138
30. Feizi, S., Cooksley, C. M., Nepal, R., Psaltis, A. J., Wormald, P. J., & Vreugde, S. (2022). Silver nanoparticles as a bioadjuvant of antibiotics against biofilm-mediated infections with methicillin-resistant Staphylococcus aureus and Pseudomonas aeruginosa in chronic rhinosinusitis patients. *Pathology, 54*(4), 453–459. https://doi.org/10.1016/j.pathol.2021.08.014
31. Khalil, M. A., El Maghraby, G. M., Sonbol, F. I., Allam, N. G., Ateya, P. S., & Ali, S. S. (2021). Enhanced efficacy of some antibiotics in presence of silver nanoparticles against multidrug resistant Pseudomonas aeruginosa recovered from burn wound infections. *Frontiers in Microbiology, 12*(September), 1–20. https://doi.org/10.3389/fmicb.2021.648560
32. Abdelghafar, A., Yousef, N., & Askoura, M. (2022). Zinc oxide nanoparticles reduce biofilm formation, synergize antibiotics action and attenuate Staphylococcus aureus virulence in host; an important message to clinicians. *BMC Microbiology*, *22*(1). https://doi.org/10.1186/S12866-022-02658-Z
33. Akbar, N., Aslam, Z., Siddiqui, R., Shah, M. R., & Khan, N. A. (2021). Zinc oxide nanoparticles conjugated with clinically-approved medicines as potential antibacterial molecules. *AMB Express, 11*(1), 1–16. https://doi.org/10.1186/s13568-021-01261-1
34. Nzilu, D. M., Madivoli, E. S., Makhanu, D. S., Wanakai, S. I., Kiprono, G. K., & Kareru, P. G. (2023). Green synthesis of copper oxide nanoparticles and its efficiency in degradation of rifampicin antibiotic. *Scientific Reports, 13*(1), 1–18. https://doi.org/10.1038/s41598-023-41119-z
35. Zhang, Y., Wang, L., Xu, X., Li, F., & Wu, Q. (2018). Combined systems of different antibiotics with nano-CuO against Escherichia coli and the mechanisms involved. *Nanomedicine, 13*(3), 339–351. https://doi.org/10.2217/nnm-2017-0290
36. Radzig, M., Nadtochenko, V., Koksharova, O. A., Kiwi, J., Lipasova, V. A., & Khmel, I. A. (2013). Antibacterial effects of silver nanoparticles on gram-negative bacteria: Influence on the growth and biofilms formation, mechanisms of action. *Colloids and Surfaces B: Biointerfaces, 102*, 300–306. https://doi.org/10.1016/j.colsurfb.2012.07.039
37. Nafee, N., Husari, A., Maurer, C. K., Lu, C., Rossi, De., Steinbach, A., Hartmann, R. W., Lehr, C.-M., & Schneider, M. (2014). Antibiotic-free nanotherapeutics: Ultra-small, mucus-penetrating solid lipid nanoparticles enhance the pulmonary delivery and anti-virulence efficacy of novel quorum sensing inhibitors. *Journal of Controlled Release, 192*, 131–140. https://doi.org/10.1016/j.jconrel.2014.06.055
38. Rather, M. A., Saha, D., Bhuyan, S., Jha, A. N., & Mandal, M. (2022). Quorum quenching: A drug discovery approach against Pseudomonas aeruginosa. *Microbiological Research, 264*(July), 127173. https://doi.org/10.1016/j.micres.2022.127173
39. Morris, G. M., Huey, R., Lindstrom, W., Sanner, M. F., Belew, R. K., Goodsell, D. S., & Olson, A. J. (2009). AutoDock4 and AutoDockTools4: Automated docking with selective receptor flexibility. *Journal of Computational Chemistry, 30*(16), 2785–2791. https://doi.org/10.1002/jcc.21256
40. Benkert, P., Biasini, M., & Schwede, T. (2011). Toward the estimation of the absolute quality of individual protein structure models. *Bioinformatics, 27*(3), 343–350. https://doi.org/10.1093/bioinformatics/btq662
41. Waterhouse, A., Bertoni, M., Bienert, S., Studer, G., Tauriello, G., Gumienny, R., Heer, F. T., de Beer, T. A. P., Rempfer, C., Bordoli, L., Lepore, R., & Schwede, T. (2018). SWISS-MODEL: Homology modelling of protein structures and complexes. *Nucleic Acids Research, 46*(W1), W296–W303. https://doi.org/10.1093/nar/gky427
42. Chen, V. B., Arendall, W. B., Headd, J. J., Keedy, D. A., Immormino, R. M., Kapral, G. J., Murray, L. W., Richardson, J. S., & Richardson, D. C. (2010). MolProbity: All-atom structure validation for macromolecular crystallography. *Acta Crystallographica Section D: Biological Crystallography, 66*(1), 12–21. https://doi.org/10.1107/S0907444909042073
43. Colovos, C., & Yeates, T. O. (1993). Verification of protein structures: Patterns of nonbonded atomic interactions. *Protein Science, 2*(9), 1511–1519. https://doi.org/10.1002/pro.5560020916
44. Jendele, L., Krivak, R., Skoda, P., Novotny, M., & Hoksza, D. (2019). PrankWeb: A web server for ligand binding site prediction and visualization. *Nucleic Acids Research, 47*(W1), W345–W349. https://doi.org/10.1093/nar/gkz424
45. Ilangovan, A., Fletcher, M., Rampioni, G., Pustelny, C., Rumbaugh, K., Heeb, S.; Cámara, M.; Truman, A.; Chhabra, S.R.; Emsley, J., Williams, P. (2013). Structural basis for native agonist and synthetic inhibitor recognition by the Pseudomonas aeruginosa quorum sensing regulator PqsR (MvfR). *PLoS Pathogens*, *9*(7). https://doi.org/10.1371/JOURNAL.PPAT.1003508
46. Majumdar, M., Dubey, A., Goswami, R., Misra, T. K., & Roy, D. N. (2020). In vitro and in silico studies on the structural and biochemical insight of anti-biofilm activity of andrograpanin from Andrographis paniculata against Pseudomonas aeruginosa. *World Journal of Microbiology and Biotechnology*, *36*(10). https://doi.org/10.1007/S11274-020-02919-X
47. Rex, D., Saptami, K., Chandrasekaran, J., & Rekha, P. (2022). Pleotropic potential of quorum sensing mediated N-acyl homoserine lactones (AHLs) at the LasR and RhlR receptors of Pseudomonas aeruginosa. https://doi.org/10.21203/rs.3.rs-1846281/v1
48. Kumar, L., Patel, S. K. S., Kharga, K., Kumar, R., Kumar, P., Pandohee, J., Kulshresha, S., Harjai, K., & Chhibber, S. (2022). Molecular mechanisms and applications of N-acyl homoserine lactone-mediated quorum sensing in bacteria. *Molecules, 27*(21), 7584. https://doi.org/10.3390/molecules27217584
49. Hanwell, M. D., Curtis, D. E., Lonie, D. C., Vandermeerschd, T., Zurek, E., & Hutchison, G. R. (2012). Avogadro: An advanced semantic chemical editor, visualization, and analysis platform. *Journal of Cheminformatics*, *4*(8). https://doi.org/10.1186/1758-2946-4-17
50. Morris, G. M., Huey, R., & Olson, A. J. (2008). Using AutoDock for ligand-receptor docking. *Current Protocols in Bioinformatics*, *24*(1). https://doi.org/10.1002/0471250953.bi0814s24

51. Yuan, S.; Chan, H.C.S.; Hu, Z. (2017). Using PyMOL as a platform for computational drug design. *Wiley Online Library*, *7*(2). https://doi.org/10.1002/wcms.1298
52. Pawar, S. S., & Rohane, S. H. (2021). Review on discovery studio: An important tool for molecular docking. *Asian Journal Of Research in Chemistry, 14*(1), 1–3. https://doi.org/10.5958/0974-4150.2021.00014.6
53. Mujwar, S., & Pardasani, K. R. (2015). Prediction of riboswitch as a potential drug target and design of its optimal inhibitors for Mycobacterium tuberculosis. *International Journal of Computational Biology and Drug Design, 8*(4), 326. https://doi.org/10.1504/IJCBDD.2015.073671
54. Mujwar, S., & Kumar, V. (2020). Computational drug repurposing approach to identify potential fatty acid-binding protein-4 inhibitors to develop novel antiobesity therapy. *Assay and Drug Development Technologies, 18*(7), 318–327. https://doi.org/10.1089/ADT.2020.976
55. Shukla, A., Shukla, G., Parmar, P., Patel, B., Goswami, D., & Saraf, M. (2021). Exemplifying the next generation of antibiotic susceptibility intensifiers of phytochemicals by LasR-mediated quorum sensing inhibition. *Scientific Reports, 11*(1), 1–23. https://doi.org/10.1038/s41598-021-01845-8
56. Kanak, K. R., Dass, R. S., & Pan, A. (2023). Anti-quorum sensing potential of selenium nanoparticles against LasI/R, RhlI/R, and PQS/MvfR in Pseudomonas aeruginosa: A molecular docking approach. *Frontiers in Molecular Biosciences, 10*(August), 1–19. https://doi.org/10.3389/fmolb.2023.1203672
57. Kotrange, H., Najda, A., Bains, A., Gruszecki, R., Chawla, P., & Tosif, M. M. (2021). Metal and metal oxide nanoparticle as a novel antibiotic carrier for the direct delivery of antibiotics. *International Journal of Molecular Sciences*, *22*(17). https://doi.org/10.3390/ijms22179596
58. Divya, M., Chen, J., Durán-Lara, E. F., Kim, K., & Vijayakumar, S. (2024). Revolutionizing healthcare: Harnessing nano biotechnology with zinc oxide nanoparticles to combat biofilm and bacterial infections-A short review. *Microbial Pathogenesis, 191*, 106679. https://doi.org/10.1016/j.micpath.2024.106679
59. Slavin, Y. N., Asnis, J., Häfeli, U. O., & Bach, H. (2017). Metal nanoparticles: Understanding the mechanisms behind antibacterial activity. *Journal of Nanobiotechnology*. https://doi.org/10.1186/s12951-017-0308-z
60. Leach, A. R., Shoichet, B. K., & Peishoff, C. E. (2006). Docking and scoring perspective. *Journal of Medicinal Chemistry, 49*(20), 5851–5855. https://doi.org/10.1021/jm060999m
61. Li, Q., Mao, S., Wang, H., Ye, X. (2022). The molecular architecture of Pseudomonas aeruginosa quorum-sensing inhibitors. *Marine Drugs*. Retrieved from https://www.mdpi.com/1660-3397/20/8/488
62. Gould, A., Schweizer, H. P., Churchill, M. E. A., Gould, T. A., Schweizer, H. P., & Churchill, M. E. A. (2004). Structure of the Pseudomonas aeruginosa acyl-homoserinelactone synthase LasI. *Wiley Online Library, 53*(4), 1135–1146. https://doi.org/10.1111/j.1365-2958.2004.04211.x
63. Shah, S., Gaikwad, S., Nagar, S., Kulshrestha, S., Vaidya, V., Nawani, N., & Pawar, S. (2019). Biofilm inhibition and anti-quorum sensing activity of phytosynthesized silver nanoparticles against the nosocomial pathogen Pseudomonas aeruginosa. *Biofouling, 35*(1), 34–49. https://doi.org/10.1080/08927014.2018.1563686
64. Mishra, A., & Mishra, N. (2021). Antiquorum sensing activity of copper nanoparticle in Pseudomonas aeruginosa: An in silico approach. *Proceedings of the National Academy of Sciences India Section B - Biological Sciences, 91*(1), 29–36. https://doi.org/10.1007/S40011-020-01193-Z
65. Vetrivel, A., Natchimuthu, S., Subramanian, V., & Murugesan, R. (2021). High-throughput virtual screening for a new class of antagonist targeting LasR of Pseudomonas aeruginosa. *ACS Omega, 6*(28), 18314–18324. https://doi.org/10.1021/acsomega.1c02191
66. Rathinam, P., Vijay Kumar, H. S., & Viswanathan, P. (2017). Eugenol exhibits anti-virulence properties by competitively binding to quorum sensing receptors. *Biofouling, 33*(8), 624–639. https://doi.org/10.1080/08927014.2017.1350655
67. Qais, F. A., Khan, M. S., Ahmad, I., Husain, F. M., Khan, R. A., Hassan, I., Shahzad, S. A., & Alharbi, W. (2021). Coumarin exhibits broad-spectrum antibiofilm and antiquorum sensing activity against gram-negative bacteria: In vitro and in silico investigation. *ACS Omega, 6*(29), 18823–18835. https://doi.org/10.1021/ACSOMEGA.1C02046
68. Pattnaik, S. S., Ranganathan, S., Ampasala, D. R., Syed, A., Ameen, F., & Busi, S. (2018). Attenuation of quorum sensing regulated virulence and biofilm development in Pseudomonas aeruginosa PAO1 by Diaporthe phaseolorum SSP12. *Microbial Pathogenesis, 118*, 177–189. https://doi.org/10.1016/j.micpath.2018.03.031
69. Churchill, M. E. A., & Chen, L. (2011). Structural basis of acyl-homoserine lactone-dependent signaling. *Chemical Reviews, 111*(1), 68–85. https://doi.org/10.1021/cr1000817
70 Prateeksha, Rao, C. V., Das, A. K., Barik, S. K., & Singh, B. N. (2019). ZnO/curcumin nanocomposites for enhanced inhibition of Pseudomonas aeruginosa virulence via LasR-RhlR quorum sensing systems. *Molecular Pharmaceutics, 16*(8), 3399–3413. https://doi.org/10.1021/acs.molpharmaceut.9b00179
71. SybiyaVasanthaPackiavathy, I. A., Agilandeswari, P., Musthafa, K. S., Karutha Pandian, S., & Veera Ravi, A. (2012). Antibiofilm and quorum sensing inhibitory potential of Cuminum cyminum and its secondary metabolite methyl eugenol against Gram negative bacterial pathogens. *Food Research International, 45*(1), 85–92. https://doi.org/10.1016/j.foodres.2011.10.022
72. Saleh, M. M., Sadeq, R. A., Abdel Latif, H. K., Abbas, H. A., & Askoura, M. (2019). Zinc oxide nanoparticles inhibits quorum sensing and virulence in Pseudomonas aeruginosa. *African Health Sciences, 19*(2), 2043. https://doi.org/10.4314/ahs.v19i2.28
73. Cui, B., Chen, X., Guo, Q., Song, S., Wang, M., Liu, J., & Deng, Y. (2022). The cell–cell communication signal indole controls the physiology and interspecies communication of Acinetobacter baumannii. *American Society for Microbiology*, *10*(4). https://doi.org/10.1128/spectrum.01027-22
74. Pu, J., Zhang, S., He, X., Zeng, J., Shen, C., Luo, Y., Li, H., Long, Y. Liu, J., Xiao, Q., Lu, Y., Huang, B., Chen, C. (2022). The small RNA AmiL regulates quorum sensing-mediated virulence in Pseudomonas aeruginosa PAO1. *American Society for Microbiology*, *10*(2). https://doi.org/10.1128/spectrum.02211-21
75. Mohajeri, M., Bayati, M., Nejad Ebrahimi, S., & Gholamnia, M. (2022). Naturally occurring quorum sensing inhibitors for Pseudomonas aeruginosa by molecular modeling. *Biointerface Research in Applied Chemistry, 13*(2), 147. https://doi.org/10.33263/BRIAC132.147
76. Ochsner, U. A., Koch, A. K., Fiechter, A., & Reiser, J. (1994). Isolation and characterization of a regulatory gene affecting rhamnolipid biosurfactant synthesis in Pseudomonas aeruginosa. *Journal of Bacteriology, 176*(7), 2044–2054. https://doi.org/10.1128/JB.176.7.2044-2054.1994
77. Pearson, J. P., Passador, L., Iglewski, B. H., & Greenberg, E. P. (1995). A second N-acylhomoserine lactone signal produced by Pseudomonas aeruginosa. *Proceedings of the National Academy of Sciences of the United States of America, 92*(5), 1490–1494. https://doi.org/10.1073/PNAS.92.5.1490
78. Borgert, S. R., Henke, S., Witzgall, F., Schmelz, S., Lage, S., Hotop, S., Stephen, S., Lübken, D., Krüger, J., Gomez, N.O., Van. Ham. M., Jänsch, L., Kalesse, M., Pich, A., Brönstrup, M., Häussler, S., Blankenfeldt, W. (2022). Moonlighting chaperone

activity of the enzyme PqsE contributes to RhlR-controlled virulence of Pseudomonas aeruginosa. *Nature Communications*, *13*(1). https://doi.org/10.1038/s41467-022-35030-w
79. Ji, H., Zhao, L., Lv, K., Zhang, Y., Gao, H., Gong, Q., & Yu, W. (2023). Citrinin is a potential quorum sensing inhibitor against Pseudomonas aeruginosa. *Marine Drugs*, *21*(5). https://doi.org/10.3390/md21050296
80. Lin, J., & Cheng, J. (2019). Quorum sensing in Pseudomonas aeruginosa and its relationship to biofilm development. *ACS Symposium Series*, *1323*, 1–16. chapter. https://doi.org/10.1021/bk-2019-1323.ch001
81. Saeki EK, Martins HM, Camargo L, Anversa L, Tavares ER, Yamada-Ogatta SF, Lioni LMY, Kobayashi RKT, Nakazato G. (2022). Effect of biogenic silver nanoparticles on the quorum-sensing system of pseudomonas aeruginosa PAO1 and PA14. *mdpi.com*. https://doi.org/10.3390/microorganisms10091755
82. Shaker, B., Ahmad, S., Thai, T. D., Eyun, S. Il, & Na, D. (2020). Rational drug design for Pseudomonas aeruginosa PqsA enzyme: An in silico guided study to block biofilm formation. *Frontiers in Molecular Biosciences*, *7*. https://doi.org/10.3389/FMOLB.2020.577316/FULL
83. Storz, M. P., Maurer, C. K., Zimmer, C., Wagner, N., Brengel, C., de Jong, J. C., Lucas, S., Müsken, M., Häussler, S., Steinbach, A., & Hartmann, R. W. (2012). Validation of PqsD as an anti-biofilm target in pseudomonas aeruginosa by development of small-molecule inhibitors. *Journal of the American Chemical Society, 134*(39), 16143–16146. https://doi.org/10.1021/ja3072397
84. Wade, D. S., Calfee, M. W., Rocha, E. R., Ling, E. A., Engstrom, E., Coleman, J. P., & Pesci, E. C. (2005). Regulation of Pseudomonas quinolone signal synthesis in Pseudomonas aeruginosa. *Journal of Bacteriology, 187*(13), 4372–4380. https://doi.org/10.1128/JB.187.13.4372-4380.2005
85. Qais, F. A., Khan, M. S., & Ahmad, I. (2019). Broad-spectrum quorum sensing and biofilm inhibition by green tea against gram-negative pathogenic bacteria: Deciphering the role of phytocompounds through molecular modelling. *Microbial Pathogenesis, 126*, 379–392. https://doi.org/10.1016/j.micpath.2018.11.030
86. Bernier, S. P., Ha, D. G., Khan, W., Merritt, J. H., & O'Toole, G. A. (2011). Modulation of Pseudomonas aeruginosa surface-associated group behaviors by individual amino acids through c-di-GMP signaling. *Research in Microbiology, 162*(7), 680–688. https://doi.org/10.1016/j.resmic.2011.04.014
87. Kolodkin-Gal, I., Romero, D., Cao, S., Clardy, J., Kolter, R., & Losick, R. (2010). D-Amino acids trigger biofilm disassembly. *Science, 328*(5978), 627–629. https://doi.org/10.1126/science.1188628
88. Ferreira De Freitas, R., & Schapira, M. (2017). A systematic analysis of atomic protein-ligand interactions in the PDB. *MedChemComm, 8*(10), 1970–1981. https://doi.org/10.1039/c7md00381a
89. Nain, Z., Sayed, S. B., Karim, M. M., Islam, M. A., & Adhikari, U. K. (2020). Energy-optimized pharmacophore coupled virtual screening in the discovery of quorum sensing inhibitors of LasR protein of Pseudomonas aeruginosa. *Journal of Biomolecular Structure and Dynamics, 38*(18), 5374–5388. https://doi.org/10.1080/07391102.2019.1700168
90. Singh, B. N., Prateeksha, Upreti, D. K., Singh, B. R., Defoirdt, T., Gupta, V. K., Souza, D. A. O., Singh, H. B., Barreira, J. C., & Vahabi, K. (2017). Bactericidal, quorum quenching and anti-biofilm nanofactories: A new niche for nanotechnologists. *Critical Reviews in Biotechnology, 37*(4), 525–540. https://doi.org/10.1080/07388551.2016.1199010
91. Borkotoky, S., Meena, C. K., & Murali, A. (2016). Interaction analysis of T7 RNA polymerase with heparin and its low molecular weight derivatives - An In silico approach. *Bioinformatics and Biology Insights, 10*, 155–166. https://doi.org/10.4137/BBI.S40427
92. Moradi, M., Gholipour, H., Sepehri, H., Attari, F., Delphi, L., Arefian, E., & Moridi Farimani, M. (2020). Flavonoid calycopterin triggers apoptosis in triple-negative and ER-positive human breast cancer cells through activating different patterns of gene expression. *Naunyn-Schmiedeberg's Archives of Pharmacology, 393*(11), 2145–2156. https://doi.org/10.1007/S00210-020-01917-Y
93. Liu, W. S., Wang, R. R., Sun, Y. Z., Li, W. Y., Li, H. L., Liu, C. L., Ma, Y., & Wang, R. L. (2019). Exploring the effect of inhibitor AKB-9778 on VE-PTP by molecular docking and molecular dynamics simulation. *Journal of Cellular Biochemistry, 120*(10), 17015–17029. https://doi.org/10.1002/JCB.28963